Commensurate, Incommensurate, and Rotated Xe Monolayers on Pt(111): A He Diffraction Study

Klaus Kern, Rudolf David, Robert L. Palmer, and George Comsa

Institut für Grenzflächenforschung und Vakuumphysik, Kernforschungsanlage-Jülich, D-5170 Jülich, West Germany

(Received 30 September 1985)

Commensurate, incommensurate, and incommensurate-rotated Xe monolayers are shown to exist on Pt(111), i.e., on a close-packed "smooth" metal surface. The existence of a commensurate-incommensurate transition induced by varying temperature at constant coverage is experimentally demonstrated ($T_{IC} = 57$–59 K). The use of high-resolution He diffraction makes possible the investigation of structures and transitions of 2D phases irrespective of the nature of the substrate and without any damaging of the adsorbed phase.

PACS numbers: 68.35.Bs, 61.16.Fk, 64.70.Kb, 79.20.Rf

The number of experimental and theoretical investigations of properties of two-dimensional (2D) phases physisorbed on crystalline substrates has increased dramatically in the last few years. This is especially true for the properties of the commensurate (C), incommensurate (I), and incommensurate-rotated (R) phases and the transitions in between.[1–6] Most of these studies are focused on the "magic" system krypton/graphite (Kr/Gr), the only system for which all three phases C, I, and R have been observed so far. By demonstrating here that the system Xe/Pt(111) also exhibits the three phases, we show that the simultaneous investigation of these phases and their mutual transitions may be extended to a large class of systems, rare gases/metal surfaces.

The C-I and I-R transitions observed so far were obtained exclusively by variation of the adsorbate coverage. (In those cases where the temperature was varied, it was done in the presence of a 3D equilibrium pressure in order to change the coverage.) Gordon and Villain[7] recently showed that anharmonic effects (different thermal expansion of adlayer and substrate) favor an I phase below a critical temperature T_{IC} and thus, in particular for Kr/Gr, they predicted a phase transition at $T_{IC} \approx 34$ K. We present here the first experimental evidence for such a C-I phase transition obtained by a simple temperature variation at constant coverage. For Xe/Pt(111), $T_{IC} \approx 57$–59 K.

The popularity of graphite as a substrate in direct structural studies of 2D adsorbed phases has obvious experimental reasons. Adsorbed monolayers can be properly investigated with neutron, high-energy electron, and synchrotron x-ray diffraction when substrate atoms like carbon with very low scattering cross sections are used; most interesting metallic substrates, like Pt, lead to obvious complications. While low-energy electron diffraction (LEED) has a greatly reduced interaction with the substrate, multiple scattering involving atoms of both adsorbate and substrate still complicates the interpretation of diffraction patterns. A more serious drawback of LEED is the large cross section for electron-stimulated desorption in most rare-gas/metal systems. The total coverage and the possible occupation of specific sites can be influenced in an uncontrollable way. The diffraction of monochromatic, highly collimated, thermal-energy He beams used here for the study of 2D phases of Xe/Pt(111) has none of these drawbacks. The possibility of getting away from the "prototype" graphite substrate[2,3,5,6] not only opens the way for more general conclusions, but allows for the use of crystals with nearly 2 orders of magnitude less broad mosaic structure. Indeed, the out-of-plane mosaic of the "single crystal" used recently in Kr/Gr synchrotron x-ray diffraction studies was $\sim 3°$ FWHM.[6] In contrast, the mosaic structure of well grown metal crystals is much narrower; in particular, for Pt crystals of the type used in this work, the mosaic FWHM is of the order of 90–100 sec of arc.

The data presented below were obtained through the use of an 18.3-meV He beam originating from a nozzle source; source and time-of-flight beam characterization were described previously.[8] The corresponding wavelength, $\lambda = 1.06$ Å, and the monochromaticity $\Delta\lambda/\lambda < 1\%$ were confirmed here by the position and width of the $(\bar{1},\bar{1})_{Pt}$ diffraction peak of the clean Pt(111) surface. Both the angular spread of the incident beam and the angle subtended by the ionizer opening are equal to 0.2°; the He beam cross section at the surface position is 3.4 mm^2. The instrumental transfer width estimated from these values and for $\varphi_f = 63.2°$ [the location of $(\bar{1},\bar{1})_{Pt}$, Fig. 1] is about 200 Å. Source and detector (quadrupole mass spectrometer) being immobile, the total scattering angle is fixed, i.e., $\varphi_i + \varphi_f = 90°$, where φ_i and φ_f are the incident and scattering angle measured from the surface normal.

The quality of the Xe layer depends critically on the density of defects and impurities on the Pt surface. The Pt(111) surface was obtained by careful orientation, cutting, and polishing.[9] Repeated sputtering, oxygen and thermal cleanings, as well as annealing cycles finally yield a surface with a defect density less than

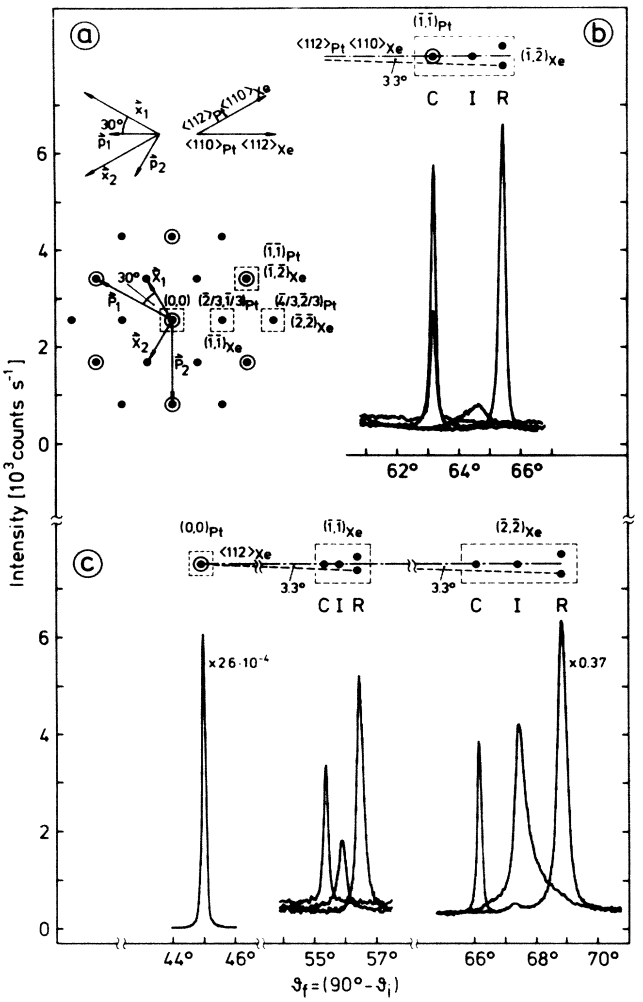

FIG. 1. Polar scans of He diffraction from clean and Xe-covered Pt(111). (a) Real- and reciprocal-space representations; $\mathbf{p}_i$ and $\mathbf{x}_i$ are the real-space and $\mathbf{P}_i$ and $\mathbf{X}_i$ the reciprocal-space basis vectors of the Pt(111) surface and of the commensurate $(\sqrt{3}\times\sqrt{3})R30°$ Xe lattice, respectively; the indexed dashed squares mark the diffraction peaks plotted. (b) Polar scan of the $(\bar{1},\bar{1})_{Pt}$ and of the $(\bar{1},\bar{2})_{Xe}$ commensurate (C), incommensurate (I), and incommensurate-rotated (R) peaks. (c) Polar scan of the $(0,0)_{Pt}$ and of the $(\bar{1},\bar{1})_{Xe}$ and $(\bar{2},\bar{2})_{Xe}$ C, I, and R peaks.

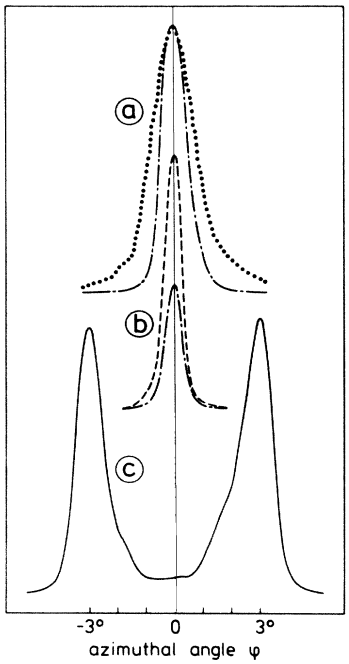

FIG. 2. Azimuthal profiles of He diffraction peaks from clean and Xe-covered Pt(111): (a) $(\bar{1},\bar{1})_{Xe}$ I (dotted) and C (dash-dotted); (b) $(\bar{1},\bar{1})_{Pt}$ (dashed) and $(\bar{1},\bar{2})_{Xe}$ C (dash-dotted); (c) $(\bar{2},\bar{2})_{Xe}$ R (solid). All peaks are normalized to the same height except for $(\bar{1},\bar{2})_{Xe}$ C which has the real relative height with respect to $(\bar{1},\bar{1})_{Pt}$.

0.1%.[10] The control of this aimed final surface state goes beyond the capabilities of current LEED and Auger spectroscopy. We have used to this end He-beam interferometry and reflectivity measurements as previously described.[10,11] The sample temperature could be varied between $25 < T_s < 1800$ K.

The base pressure with the He beam off was in the low 10^{-11}-mbar range. Xe was adsorbed from the gas phase at pressures around 10^{-8} mbar. For Figs. 1, 2, and 4, when the desired coverage was reached, the 3D Xe gas was pumped away. The adsorbed layers were carefully annealed until an optimal equilibrium structure was obtained. In all cases T_s was low enough so that no Xe coverage reduction could be detected during the measurement. The average Xe coverage θ, defined with respect to the density of Pt atoms in the topmost layer (1.50×10^{15} cm^{-2}), is estimated up to $\theta = 0.25$ from the Xe exposure. In the present work, only the local coverage within the diffracting Xe islands is really relevant. This value is obtained from the lattice parameters deduced from polar patterns like those in Fig. 1. None of the Xe phases discussed here have atoms in the second layer. This was checked very accurately by surface phonon spectroscopy.[12]

The polar and azimuthal scans shown in Figs. 1 and 2, respectively, characterize the structure of the three Xe phases observed on Pt(111). The real- and reciprocal-space representations of the Pt(111) and a $(\sqrt{3}\times\sqrt{3})R30°$ adlayer structure are shown in Fig. 1(a). The reciprocal lattice points corresponding to the diffraction peaks shown in Figs. 1(b) and 1(c) are enclosed in dashed squares. The lattice points are indexed with respect to the reciprocal basis vectors of the Pt substrate ($\mathbf{P}_i$) as usual and also of the adlayer ($\mathbf{X}_i$). In the presence of an adlayer there are no "substrate" peaks in the He diffraction patterns and thus the $\mathbf{X}_i$ indexing is more appropriate. Above each of the group of peaks in Figs. 1(b) and 1(c) the corre-

sponding dashed squares are shown again; the relative positions of the diffraction peaks of the clean Pt substrate (open circles) and of the three C, I, and R phases of the Xe layer (filled circles) are represented schematically within each square. All peaks shown in Figs. 1 and 2 are measured at $T_s = 25$ K except for the C peaks measured at 64 K.

Two diffraction peaks of the clean Pt(111) surface are plotted in Figs. 1 and 2: the specular $(0,0)_{Pt}$ peak in Fig. 1(c) and the $(\bar{1},\bar{1})_{Pt}$ peak in Fig. 1(b) (polar scan) and in Fig. 2(b) (azimuthal scan). The height of the $(\bar{1},\bar{1})_{Pt}$ peak is about 2.3×10^{-4} times the height of the $(0,0)_{Pt}$ peak. [The $(\bar{2},\bar{1})_{Pt}$ peak, not shown, is also seen; its height is about 10^{-5} times the height of the $(0,0)_{Pt}$ peak.] The average terrace widths being larger than 2000 Å,[10] i.e., more than ten times the estimated transfer width, the shapes of the $(\bar{1},\bar{1})_{Pt}$ peak in Figs. 1(b) and 2(b) are fully determined by the instrument; the corresponding experimental transfer widths are 250 and 180 Å, respectively, in fair agreement with the estimation. These widths will be used below to analyze the corresponding peak profiles of the Xe phases.

The Xe C-phase diffraction peaks shown in Figs. 1(b), 1(c), 2(a), and 2(b) are present in the whole $\theta < 0.33$ and $60\text{ K} < T_s < 99$ K range. From the peaks present and from the lattice parameter $|\mathbf{x}_i| = 4.80 \pm 0.02$ Å obtained from a large number of polar scans like those in Fig. 1, it is obvious that the C phase has a commensurate $(\sqrt{3}\times\sqrt{3})R30°$ structure. Comparison of the polar and azimuthal peak profiles of the Xe C phase—$(\bar{1},\bar{2})_{Xe}$—and of the clean Pt(111) surface—$(\bar{1},\bar{1})_{Pt}$—(the smaller and the larger peak, respectively) shows that the C-phase peak is only slightly broadened. A linear dimension of at least 500–1000 Å for the Xe C-phase domains can be estimated. The simple existence of the Xe C phase demonstrates that, contrary to a widespread belief, the corrugation of the rare-gas/close-packed-metal surface potential is strong enough to lock very effectively the C phase in spite of the appreciable strain of the Xe—Xe bond (the $\sqrt{3}d_{Pt\text{-}Pt}$ distance of 4.80 Å is 9% larger than the $d_{Xe\text{-}Xe}$ bulk next-neighbor distance at 60 K).

The peaks denoted by I in Figs. 1(b), 1(c), and 2(a) are obtained from a phase which, like the C phase, is rotated with respect to the substrate by 30° but, unlike the C phase, has a lattice vector incommensurate with low-order lattice vectors of the substrate; it is an incommensurate phase. The I phase is present in the whole range $\theta < 0.33$ up to about 55 K and in the range $0.33 \lesssim \theta \lesssim 0.38$ and $T_s < 99$ K. Also unlike the C phase, the modulus of the lattice vector $|\mathbf{x}_i|_I$ of the I phase is not constant but varies with both T_s and θ.[12] The I-peak maxima in Fig. 1(c) measured at $\theta \approx 0.3$ correspond to $|\mathbf{x}_i|_I = 4.48 \pm 0.03$ Å, i.e., to a local coverage 0.378 ± 0.005. The FWHM of the I peaks in Figs. 1(c) and 2(a) lead consistently to a linear dimension of the I domains of about 150 Å. In contrast to the C and R peaks the polar shapes of the I peaks are strongly asymmetric; the I phase appears to be less homogeneous than the other phases (see also Ref. 3 and Abraham, Rudge, and Auerbach[13]).

The azimuthal plot in Fig. 2(c) shows that the R phase consists of domains rotated from the common orientation of the C and I phases (there is of course no "left" or "right" preference). The existence of the incommensurate-rotated R phase was predicted by Novaco and McTague[4] and was seen for rare gases on graphite and alkali atoms[14,15] on metal but so far not for rare gases on close-packed metal surfaces. The rotation angle of 3.3° [Fig. 2(c)] at a misfit of $10.4\% \pm 0.06\%$ as deduced from the location of the corresponding R peaks in Figs. 1(b) and 1(c) ($|\mathbf{x}_i| = 4.30 \pm 0.03$ Å) is in reasonable agreement with the prediction. The deduced coverage, $\theta = 0.416 \pm 0.06$, is the highest monolayer coverage reached at this temperature. The average domain width of the R phase of about 250 Å and the symmetric polar shape of the R peaks indicate that the "incommensurate" R phase is nearly as well locked as the C phase. This suggests that an analysis of the type proposed by Fuselier, Raich, and Gillis[16] and Doering[14] might be successful. It is particularly interesting, in the same context, that the I phase is less well ordered than the R phase, although the average binding of the Xe atoms to the surface appears to be substantially reduced in the R phase.[12]

The growth of the Xe phases during Xe adsorption ($p_{Xe} = 8\times10^{-9}$ mbar) at constant temperature is exemplified in Fig. 3. Each of the three phases is followed separately by monitoring of the detector counting rate versus exposure time. The scattering

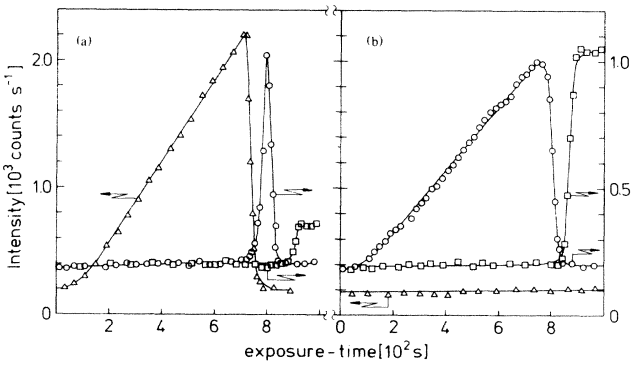

FIG. 3. Peak height of $(\bar{1},\bar{1})_{Xe}$ C (triangles), I (circles), and R (squares) vs Xe exposure time at constant temperature: (a) 64 K; (b) 50 K.

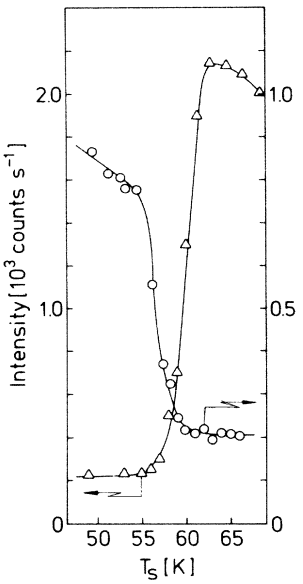

FIG. 4. Peak height of $(\bar{1},\bar{1})_{Xe}$ C (triangles) and I (circles) vs temperature at constant Xe coverage, $\theta \approx 0.3$.

geometry is set in each case at one of the positions corresponding to the C, I, or R $(\bar{1},\bar{1})_{Xe}$ peaks, respectively. At coverages $\theta < 0.33$ either the C phase (triangles) (at $T_s = 64$ K $> T_{IC}$) or the I phase (circles) (at $T_s = 50$ K $< T_{IC}$) is stable; after a short induction period the corresponding intensity increases almost linearly. The induction period is due to the diffuse scattering of the He beam at the Xe islands' border. Indeed, it was recently shown[17] that in a band 12 Å wide along step edges on a Pt(111) surface there is no coherent He scattering; i.e., only islands larger than ~ 12 Å contribute to the diffraction intensity. The apparently linear increase is probably due to a fortuitous compensation between the decreasing sticking coefficient (above $\theta \sim 0.25$), the almost quadratic increase of the diffracted intensity with the average island area, and the narrowing of the peak profiles with increasing Xe island dimensions. At $T_s = 64$ K [Fig. 3(a)], when the C-phase saturation coverage ($\theta_c = 0.33$) is surpassed, the C intensity falls dramatically while the I intensity increases correspondingly and then, within a short exposure interval, I falls also sharply. With further exposure the R phase (squares) appears, reaches rapidly its maximum intensity, and remains stable. At $T_s = 50$ K [Fig. 3(b)] the disappearance of the I phase and the appearance and growth of the R phase are similar except for the much higher value of the R intensity. (The R-phase Xe atoms desorb markedly at 64 K.[12]) On the other hand, because the C phase is unstable below T_{IC}, the I phase starts to grow from the beginning of the exposure and is thus present in a large coverage range.

Finally, in Fig. 4 direct evidence for the I-C transition at constant θ is presented. The intensity diffracted from the I (circles) and C (triangles) phases is monitored as in Fig. 3, with the difference that here not T_s but θ is maintained constant by pumping off of the Xe. There is no observable hysteresis when T_s is increased or decreased. T_{IC} is estimated to be 57–59 K. The existence of this transition was predicted recently by Gordon and Villain,[7] but there was no experimental evidence so far for physisorbed monolayers.

[1]P. Bak, Rep. Prog. Phys. **45**, 587 (1982); J. Villain and M. B. Gordon, Surf. Sci. **125**, 1 (1983); *Ordering in Two Dimensions,* edited by S. K. Sinha (North-Holland, New York, 1980), and references therein.

[2]M. D. Chinn and S. C. Fain, Jr., Phys. Rev. Lett. **39**, 146 (1977).

[3]P. W. Stephens, P. A. Heiney, R. J. Birgeneau, P. M. Horn, D. E. Moncton, and G. S. Brown, Phys. Rev. B **29**, 3512 (1984).

[4]A. D. Novaco and J. P. McTague, Phys. Rev. Lett. **38**, 1286 (1977); H. Shiba, J. Phys. Soc. Jpn. **48**, 211 (1980).

[5]C. G. Shaw, S. C. Fain, Jr., and M. D. Chinn, Phys. Rev. Lett. **41**, 955 (1978).

[6]K. L. D'Amico, D. E. Moncton, E. D. Specht, R. J. Birgeneau, S. E. Nagler, and P. M. Horn, Phys. Rev. Lett. **53**, 2250 (1984).

[7]M. B. Gordon and J. Villain, J. Phys. C **18**, 3919 (1985).

[8]K. Kern, R. David, and G. Comsa, Rev. Sci. Instrum. **56**, 369 (1985).

[9]U. Linke and B. Poelsema, J. Phys. E **18**, 26 (1985).

[10]B. Poelsema, R. L. Palmer, G. Mechtersheimer, and G. Comsa, Surf. Sci. **117**, 60 (1982).

[11]G. Comsa and B. Poelsema, Appl. Phys. A **38**, 153 (1985).

[12]K. Kern, R. David, R. L. Palmer, and G. Comsa, to be published.

[13]F. F. Abraham, W. E. Rudge, D. J. Auerbach, and S. W. Koch, Phys. Rev. Lett. **52**, 445 (1984).

[14]D. L. Doering, J. Vac. Sci. Technol. A **3**, 809 (1985).

[15]T. Aruga, H. Tochihara, and Y. Murata, Phys. Rev. Lett. **52**, 1794 (1984).

[16]C. R. Fuselier, J. C. Raich, and N. S. Gillis, Surf. Sci. **92**, 667 (1980).

[17]L. K. Verheij, B. Poelsema, and G. Comsa, Surf. Sci. (to be published).